ECE 569: Topological Quantum Computation and the Kitaev Honeycomb Model

Amir Shapour Mohammadi

June 2, 2023

Abstract

In this paper, we discuss the Kitaev honeycomb model and its importance as a physical system capable of facilitating topological quantum computation. An overview of the necessary quantum statistics, braiding, and fusion of anyons will be provided. We will explore the Ising anyon model and derive that it is sufficient for universal topological quantum computation. We will then introduce the Kitaev honeycomb model and derive its decomposition into Majorana fermions. Its energy spectrum and distinct phases will be covered, and we will then discuss the presence of Ising anyons in one of its phases.

1 Anyons

1.1 Quantum statistics and anyons

We begin with a discussion of the quantum statistics of fermions and bosons which include all known particles in the Standard Model. Given the wave function of a single particle, $\psi(x)$, it is natural to ask what the wave function $\psi[x] = \psi(x_1, \ldots, x_n)$ of an n-particle system must satisfy. An important assumption is that these particles are indistinguishable. Consider exchanging 2 particles which we denote by the operator P_{ij} with action

$$P_{ij}\psi(x_1, \ldots, x_i, \ldots, x_j, \ldots, x_n) = \psi(x_1, \ldots, x_j, \ldots, x_i, \ldots, x_n). \tag{1}$$

Since the particles are indistinguishable, this exchange should not have physical consequences, and therefore the probability density of the wave function must stay invariant, or $|\psi[x]| = |P_{ij}\psi[x]|$ for all x. This therefore implies that the action of P_{ij} is to apply a scalar SU(1) factor of $e^{i\theta}$ for some θ. Due to topological considerations, the SU(1) factor must be ± 1 in 3 dimensions corresponding to bosons and fermions respectively. In 2 dimensions, there is no restriction on the SU(1) factor. Note that it is purely topological considerations which lead to these results. As we mentioned earlier, all known particles are fermions and bosons, and therefore one may ask why it is worthwhile to study these general results. It turns out in condensed matter and other related fields that so-called quasiparticles, or excitations of quantum fields due to a collection of particles, can have more exotic properties than the simple ± 1 exchange factor. Examples of quasiparticles include phonons, magnons, spinons, and composite fermions, with the last one exhibiting non-trivial quantum statistics [1].

1.2 Geometric phase

In addition to this topological SU(1) factor, geometry also plays a role in the statistics angle. Depending on the geometry of the Hilbert space, and the degeneracy of its eigenspaces, particles can pick up a so-called Berry (geometric) phase upon adiabatic change in coordinates. A more familiar geometric phase is that of the Aharonov-Bohm effect in which a particle with charge q in a magnetic vector potential $\mathbf{A}$ picks up a phase [1]

$$e^{i\phi}, \qquad \phi = \frac{q}{\hbar}\oint d\mathbf{l}\cdot\mathbf{A} = \frac{q}{\hbar}\int d\mathbf{\Sigma}\cdot\mathbf{B} \tag{2}$$

where $\mathbf{B} = \mathbf{\nabla}\times A$ is the magetic field. The Berry phase involves a similar notion in which the curvature of the Hilbert space, or more specifically its holonomy, entails a factor applied to the wave function upon adiabatic transport, even if moving around a closed loop. We will not provide a derivation for sake of brevity, but for an eigenspace with dimension n, the Adiabatic theorem implies that adiabatic transport (slow change of parameters of a Hamiltonian system) will result in a SU(n) phase

$$e^{i\Gamma}, \qquad \Gamma = \mathcal{P}\oint d\mathbf{l}\cdot\mathcal{A} = \mathcal{P}\int d\mathbf{\Sigma}\cdot\mathbf{\Omega} \tag{3}$$

where $\mathcal{A}$ denotes the Berry connection and $\mathbf{\Omega} = d\mathcal{A}$ denotes the Berry curvature of the eigenspace. In analogy with the Aharonov-Bohm effect, $\mathcal{A}, \mathbf{\Omega}$ can be thought of as the magnetic vector potential and magnetic field respectively. Here, $\mathcal{P}$ denotes path-ordering which we will not discuss. The central result is that there are quasiparticles which transform under general SU(n) transformation. It is important to note that Berry phase is not a property of the particle, but rather of the Hamiltonian, and describes the evolution of particles rather than the exchange of two particles. However, the existence of a quasiparticle may change the curvature of the Hilbert space, and therefore induce a statistical angle upon other quasiparticles which orbit it. For instance, in the fractional quantum Hall effect, there exist quasihole excitations of the quantum fluid which have anyonic statistics due to a combination of the Aharanov-Bohm effect and Berry phase. Anyons which have a non-trivial SU(1) scale factor are known abelian anyons while those which have a SU($n > 1$) factor are known as non-abelian anyons. There is also the usual dynamical phase $\varphi(t) = i/\hbar\int_0^t dt'\varepsilon(t')$ accrued by an eigenstate of the Hamiltonian, though we are less interested in this contribution.

2 Braiding of anyons

2.1 Braid Group

We can represent the pair-wise exchange of a set of n particles by the braid group $\mathcal{B}_n$. This group has generators $\{b_i\}_{i=1}^{n-1}$ which satisfy the relations $[b_i, b_j] = 0$ if $|i-j| \geq 2$ and $b_i b_{i+1} b_i = b_{i+1} b_i b_{i+1}$ known as the Yang-Baxter equations [4]. The generator b_i represents counterclockwise exchange of particles i and $i+1$. Note that in general, $b_i^2 \neq 1$ where 1 is the identity element of $\mathcal{B}_n$ and represents trivial action. The first relation $[b_i, b_j] = 0$ (for $|i-j| \geq 2$) is trivial by noting that the particles being braided are not related since they are far from each other, and therefore the order of their braiding does not matter. The second relation $b_i b_{i+1} b_i = b_{i+1} b_i b_{i+1}$ is better explained by writing out the braids on a piece of paper. We have not yet explained the action of this group on the Hilbert space. To do this we need the formalism of representation theory. In particular, we are interested in unitary $\mathbb{C}^n$ representation of the braid group, or a homomorphism $\rho : \mathcal{B}_n \to \mathrm{SU}(n)$. The homomorphism requirement is natural in that we want to preserve the group structure to form an action on the Hilbert space. In other words, the image of the generators under this representation should obey the same commutation relations as the generators themselves, and so for instance $\rho(b_i)\rho(b_{i+1})\rho(b_i) = \rho(b_{i+1})\rho(b_i)\rho(b_{i+1})$. We will briefly return to the braid group when we discuss fusion.

2.2 Fusion

We consider a system with a number of distinct particles which we label $1, a, b, c, \ldots$ where 1 corresponds to the vacuum state (may or may not refer to the non-existence of a particle). For instance, a may correspond to electrons, while b corresponds to photons, or some other particle or quasiparticle. The model must contain the antiparticles of each particle species so that annihilation to the vacuum state 1 is allowed. If we were considering an ordinary electron gas, then it would correspond to a $1, a, \overline{a}$ model where a denotes electrons and $\overline{a}$ denotes positrons (the antiparticle of electrons). We now consider how these particles interact with one another and are mainly interested in their collective behavior when pairs of them are brought together in space in a process called fusion. Interactions need not actually manifest between the particles. Fusion is purely a result of the statistics of particles. For instance, a pair of electrons bound together have the quantum statistics of a boson. To see this, note that moving one such pair completely around another pair would yield a phase of $(-1)^2 = 1$ since each of the two electrons would gain a phase factor of -1. In general, fusion involving particles a and b can be written as the product operation [4]

$$a \times b = \sum_c N_{ab}^c c \tag{4}$$

where N_{ab}^c is an integer which counts the number of distinct mechanisms which may create c. Note for instance that $a \times b = 2c$ does not mean that 2 c particles are produced from fusing a and b, but that there are 2 distinct processes for producing c. We will expand on this shortly. The fusion operator is commutative, meaning that $a \times b = b \times a$. The fusion operator is also associative. In other words, given a system of 3 particle species a, b, c, we are free to choose whether a and b fuse first and then c, or if b and c fuse first and then a, or $(a \times b) \times c = a \times (b \times c)$. We can therefore write $a \times b \times c$ since it is well-defined. Suppose that the 3 particles species have a single fusion channel d, or $a \times b \times c = d$. Although the outcome is well-defined (due to associativity), the intermediate steps need not be identical since $a \times b = i$ need not equal $b \times c = j$ and therefore a different intermediate particle was produced in the fusion to d. The so-called F matrix with elements $(F_{abc}^d)_i^j$ describes these distinct fusion processes. The order in which particles are fused can be viewed as a basis of the fusion space, and the F matrix allows one to change basis. Note that the order cannot be regarded as a gauge since the intermediate particle is an observable.

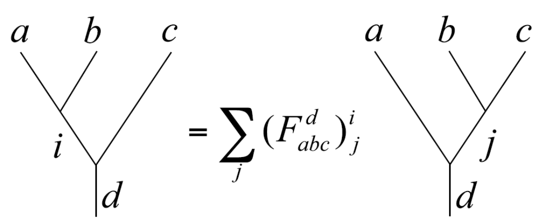

Figure 1: The diagram (and all others in this paper) is read from top to bottom. The F matrix allows us to transform between the intermediate particle of the fusion channel. We started with $(a \times b) \times c = i \times c = d$ and transformed to $a \times (b \times c) = a \times j = d$ [4].

We now return to the exchange statistics of particles. Given a deterministic fusion operation $a \times b \mapsto c$ of anyons a, b, we consider exchanging a and b. Note that this is equivalent to a half-rotation of c, and therefore the exchange evolution R_{ab}^c is a SU(1) scale factor. We can build the full R_{ab} matrix by considering the complete fusion channel of $a \times b$ and placing the scale factor R_{ab}^c on the diagonals of R_{ab} for all outcomes c. This object is referred to as the exchange matrix, or simply the R matrix and captures the exchange statistics of particles with explicit fusion outcomes. In general, we may not be in a situation where $a \times b$ corresponds to a single particle, and we must consider the more general case of a superposition of outcomes. If the fusion channels of a model all have single outcomes, then the model is called abelian since interchanging 2 particles can only yield a phase factor. On the other hand, if any of the fusion channels have multiple outcomes (e.g. $a \times b = c + d$) then the dimension of the fusion space is larger than 1, and so braiding a, b can yield non-trivial SU(2) factors. This lattice model is called non-abelian.

It becomes useful to define a more general unitary (though not necessarily diagonal) exchange matrix B which better captures the whole statistics. We have the relation between the 3 defined quantities thus far [4]

$$B_{ab} = (F^d_{acb})^{-1} R_{ab} F^d_{acb} \tag{5}$$

where B_{ab} corresponds to the factor applied by braiding a and b. The left hand side is simply the SU(n) factor from exchanging a and b directly, while the right hand side consists of the effect on the direct fusion channels of a, b. In other words, B_{ab} is the image of the appropriate generator of some irreducible representation of the braid group, and the B matrix corresponds to an irreducible representation. Note that B_{ab} implicitly depends on c, d. There are a couple restrictions that the F and R matrices must satisfy known as the pentagon and hexagon identities, though we will not cover them here.

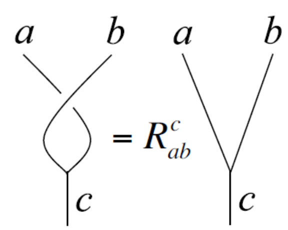

Figure 2: The R matrix allows us to exchange 2 particles prior to fusing them. Although the outcome c is the same before and after twisting, there is a phase accrued with the R matrix assigns. The R matrix is only applicable when there is a single outcome of a fusion channel [4].

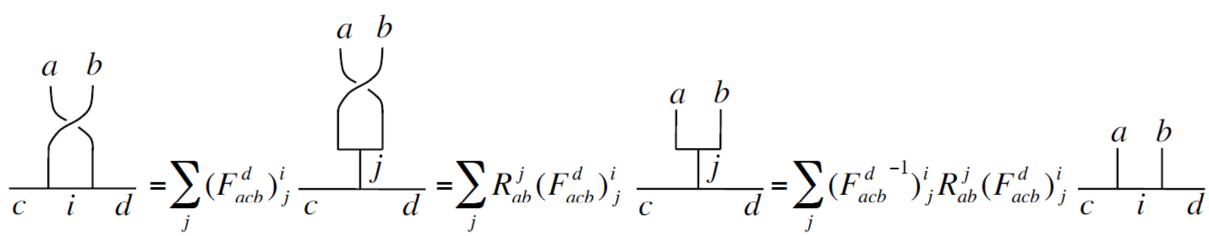

Figure 3: The B matrix allows us to exchange 2 particles when their fusion channel does not have a single outcome. The left-most diagram is the action of the B_{ab} matrix. We can re-evaluate this action by reordering the fusion using the F matrix, then untwisting the particles using the R matrix, and finally undoing the action of the F matrix to return to the original fusion [4].

2.3 Ising Anyons

We now discuss an important model of anyons and their fusion channels known as the Ising anyons. We will return to this model when we discuss the Kitaev honeycomb model. There are 2 non-trivial particles consisting of the non-abelian anyon σ and the fermion ψ. The fusion channels are given by [4]

$$\sigma \times \sigma = 1 + \psi, \qquad \sigma \times \psi = \sigma, \qquad \psi \times \psi = 1. \tag{6}$$

There are a number of implications made by these relations. Firstly, the last relation $\psi \times \psi = 1$ tells us that the fermion ψ is its own anti-particle since it can annihilate itself. In other words, ψ is a Majorana fermion. The second relation $\sigma \times \psi = \sigma$ implies that ψ leaves the anyonic properties of σ unchanged. The first relation $\sigma \times \sigma = 1 + \psi$ tells us that σ may be its own anti-particle $\sigma \times \sigma \mapsto 1$ and therefore act like a Majorana fermion or may fuse to form the ψ fermion. This model is rich in exciting phenomena which we will now discuss. Using the pentagon and hexagon identities as well as the defining relations above, we state the relevant matrices [4]

$$F^{\sigma}_{\sigma\sigma\sigma} = \frac{1}{\sqrt{2}} \begin{pmatrix} 1 & 1 \\ 1 & -1 \end{pmatrix}, \qquad R_{\sigma\sigma} = e^{-i\pi/8} \begin{pmatrix} 1 & 0 \\ 0 & i \end{pmatrix} \tag{7}$$

written in the basis $\{|(\sigma,\sigma) \mapsto 1\rangle, |(\sigma,\sigma) \mapsto \psi\rangle\}$ (we use this self-explanatory notation to indicate the fusion outcome). The F matrix above, which is the familiar Hadamard gate H, describes the intermediate particles in the fusion operation $\sigma \times \sigma \times \sigma \mapsto \sigma$, and the intermediate states are precisely the vacuum and fermion states $1, \psi$ as expected since $\sigma \times \sigma = 1 + \psi$. On the other hand, the diagonal R matrix, which is the $\sqrt{\sigma^z}$ gate, describes the exchange statistics of exhanging a pair of σ anyons during the distinct fusion operations $\sigma \times \sigma \mapsto 1, \psi$. We see that $R^{1}_{\sigma\sigma} = e^{-i\pi/8}$ and $R^{\psi}_{\sigma\sigma} = e^{i3\pi/8}$ which is reasonable since the additional $\pi/2$ phase picked up by the fermion fusion outcome is a result of the fermionic exchange statistics (recall that a full exchange picks up the factor $e^{i\pi} = -1$). We still do not know the statistics of braiding an Ising anyon σ with itself. To see this, we utilize the braid matrix [4]

$$B = FR^2F^{-1} = e^{-i\pi/4} \begin{pmatrix} 0 & 1 \\ 1 & 0 \end{pmatrix}. \tag{8}$$

Although this all sounds very exciting, it is not completely clear so far how we can utilize this

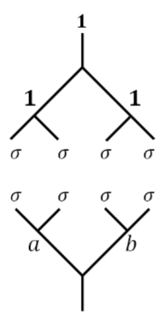

	a	b
$\|0\rangle$	**1**	**1**
$\|1\rangle$	ψ	ψ

Figure 4: Encoding 1 logical qubit using 4 Ising anyons. The top diagram shows creating the Ising anyons from the vacuum. The bottom diagram shows fusing the 4 Ising anyons into the vacuum with 2 intermediate states, $|0\rangle, |1\rangle$ as indicated in the table [3].

formalism for computation. It turns out that it is quite simple in theory. We can encode qubits in the intermediate states of the fusion process. For instance, given 4 Ising anyons σ (which we can produce from the vacuum 1), we can fuse them them back to the vacuum 1 with 2 distinct intermediate steps which we denote a, b. Since we produced the 4 Ising anyons from the vacuum,

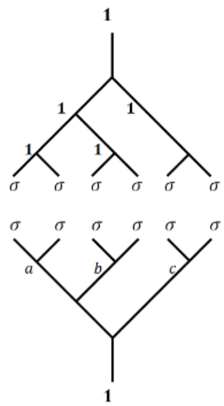

	a	b	c
$\|00\rangle$	**1**	**1**	**1**
$\|10\rangle$	ψ	ψ	**1**
$\|01\rangle$	**1**	ψ	ψ
$\|11\rangle$	ψ	**1**	ψ

Figure 5: Encoding 2 logical qubits using 6 Ising anyons. The top diagram shows creating the Ising anyons from the vacuum. The bottom diagram shows fusing the 6 Ising anyons into the vacuum with 4 intermediate states, $|00\rangle, |01\rangle, |10\rangle, |11\rangle$ as indicated in the table [3].

there is an addition restriction which we have not discussed yet. A naive consideration would conclude that there are 4 intermediate steps a, b equal to any of $1, \psi$. However, consider $a = 1, b = \psi$, then these particles could fuse to $1 \times \psi = \psi$ even though we started with the vacuum 1. In all, we transformed 1 to ψ which is not allowed. We say that the initial state of 4 Ising anyons belong to the vacuum sector. We must only consider intermediate steps which can fuse back to the vacuum state since that is where we started. Hence there are only 2 intermediate steps $a = b = 1$ and $a = b = \psi$ since $1 \times 1 = 1$ and $\psi \times \psi = 1$, but $1 \times \psi = \psi \times 1 = \psi \neq 1$. We can also encode 2 qubits using 6 Ising anyons with the same idea. In general, a system of $2N$ anyons have 2^{N-1} intermediate steps which fuse to the vacuum, and therefore encode $N - 1$ qubits.

We can braid Ising anyons (R) and change their fusion order (B) to applying logical operations. Note however that the R and B matrices do not together form a universal gate set and must be supplemented by a phase gate which can be implemented using more down-to-Earth dynamical means. Once we are able to implement the phase gate, we have obtained a method of universal topoloical quantum computation using (primarily) the braiding of Ising anyons. We will now review a well-known physical model that hosts the Ising model.

3 Kitaev Honeycomb Model

3.1 Introduction

We now consider the Kitaev honeycomb model which was theorized by Alexei Kitaev in 2005 [2]. The model consists of a honeycomb lattice with spins on the vertices. Each spin interacts with its 3 nearest neighbors which can be indexed by links connecting the vertices. There are 3 distinct links in the lattice which are denoted as x, y, z links. The spin interaction is restricted based on the link it corresponds to. For instance, spins interacting via an x link only interact with the x component of their spins, resulting in the interaction term $\sigma_i^x \sigma_j^x$ where i, j denote the (nearest neighbor) vertices. Although this spin interaction may seem unmotivated, there exist atomic lattice structures which exhibit similar interactions due to anisotropic spin-orbit coupling. This 2-dimensional (2d) spin-chain model is interesting for a number of reasons. First, we note that 1d spin-chains are exactly solvable using so-called Jordan-Wigner (JW) transformations where the spin operators are transformed to fermionic operators, and the Hamiltonian is then diagonalized. However, this method (almost always) fails to provide any significant help in tackling 2d spin-chains, except for the present model. Due to the immense number of conserved quantities in the model, the JW transformation allows us to solve the system exactly, meaning that we can compute the energy spectrum analytically. However, the JW transformation is not in terms of the usual Dirac fermions but Majorana fermions. Thus, the 2d spin-chain is converted to an exactly solvable Hamiltonian in terms of Majorana fermions with quadratic dependence on the fermion operators. There are gapped and gapless phases depending on the spin-coupling (scalar) real parameters J_x, J_y, J_z. Both abelian and Ising non-abelian anyons can manifest in particular phases, and so the model is also a theoretical candidate for universal topological quantum computing as already discussed.

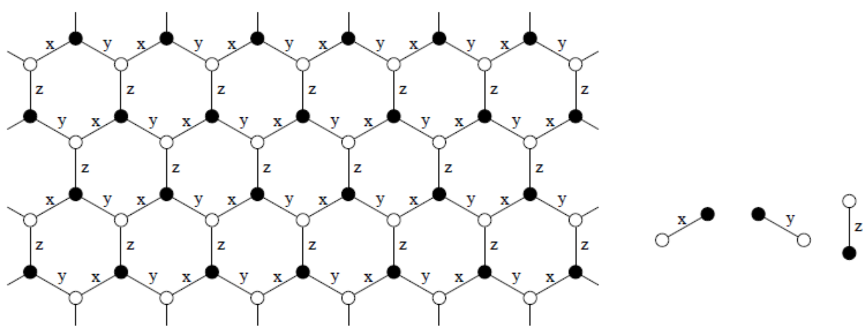

a) b)

Figure 6: Kitaev honeycomb lattice model with sublattices colored black/white, and the 3 distinct bonds x, y, z labeled [2].

We now explore this model, and derive its interesting properties closely following Kitaev's seminal paper [2]. The Hamiltonian can be written

$$H = -J_x \sum_{x \text{ links}} \sigma_j^x \sigma_k^x - J_y \sum_{y \text{ links}} \sigma_j^y \sigma_k^y - J_z \sum_{z \text{ links}} \sigma_j^z \sigma_k^z \tag{9}$$

where σ_a^b is the σ^b Pauli matrix for site a. The products of spin operators are actually tensor products $\sigma_j^a \otimes \sigma_k^b$ which we omit for shorthand. We call each honeycomb cell a plaquette and label the 6 lattice sites $1, \ldots, 6$. If 2 plaquettes are neighbors then they share 2 vertices, and otherwise then they share no vertices. For plaquette p, we define the plaquette operator

$$W_p = \sigma_1^x \sigma_2^y \sigma_3^z \sigma_4^x \sigma_5^y \sigma_6^z. \tag{10}$$

The plaquette operator is written as the product of the spin operators of the sites where for each site we take the spin operator corresponding to the link perpendicular to the plaquette. This operator will be crucial to our simplification of the Hamiltonian. It is a simple computation to confirm that $[W_i, W_j] = 0$ for any i, j due to the anti-commutation relations of the Pauli matrices. In addition, $[H, W_i] = 0$, and therefore each plaquette operator W_i is a constant of motion of the system. Note that the plaquette operators obey the condition $W_i^2 = 1$ and therefore have eigenvalues $w_i = \pm 1$. Thus, the Hamiltonian can be diagonalized in blocks of eigenspaces of the plaquette operators. More explicitly, if $\mathcal{H}$ denotes the total Hilbert space, and $\mathcal{H}_{[w_i]}$ denotes the eigenspace or sector associated with eigenvalues $[w_i] = (w_1, w_2, \ldots)$, then we have the decomposition $\mathcal{H} = \bigoplus_{[w_i]} \mathcal{H}_{[w_i]}$.

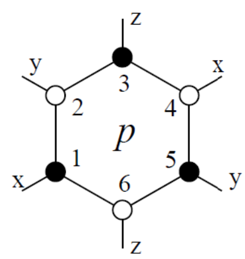

Figure 7: The plaquette refers to a single honeycomb with vertices labeled. The plaquette operator W_p is defined as the product of the bonds labelled here, with vertices identified [2].

The ground state then belows to some $\mathcal{H}_{[w_i]}$ and so we can restrict our attention to that space. In fact, it turns out that the ground state belongs to the $[w_i] = (1, 1, \ldots)$ sector known as the vortex-free sector where vortices refer to spaces with $w_i = -1$ for some i. We will return to this notion.

3.2 Jordan-Wigner transformation into Majorana fermions

We now map this 2d spin-chain to a problem of Majorana fermions via a so-called Jordan-Wigner transformation. The fermions that we are familiar with (those that are not their own anti-particles) are known as Dirac fermions and have creation and annihilation operators $a_i^\dagger, a_i$ respectively. These operators satisfy the anti-commutation relations $\{a_i, a_j^\dagger\} = \delta_{ij}$, $\{a_i, a_j\} = 0$. A particle is its own anti-particle if and only if its creation and annihilation operators are Hermitian conjugates of one another, or $a = a^\dagger$. Majorana fermions are their own anti-particles while Dirac fermions are not. We can define Majorana fermion operators c in terms of Dirac fermion operators a by expressing

$$c_{2j-1} = a_j + a_j^\dagger, \qquad c_{2j} = -i(a_j - a_j^\dagger) \tag{11}$$

for $k = 1, \ldots, n$. These operators satisfy the relations $c_j^2 = 1$, $\{c_i, c_j\} = 0$ for $i \neq j$, and are

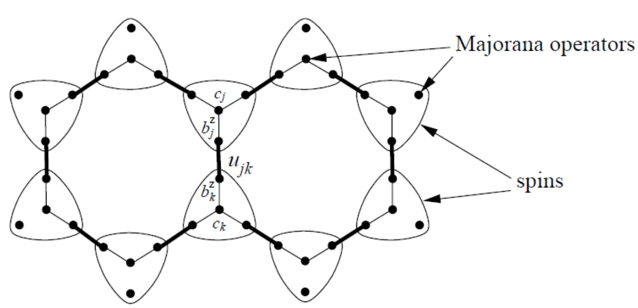

Figure 8: The decomposition of plaquettes into Majorana fermions. The spin on each vertex has been transformed into 4 Majorana fermions which are labeled here. Majorana fermions of adjacent vertices can then make bonds as indicated $\hat{u}_{jk} \propto b_j^z b_k^z$ [2].

Hermitian. We can also represent the spin operators by 2 (Dirac) fermionic modes, or 4 Majorana modes which we denote by b^x, b^y, b^z, c, where c is not related to the Majorana fermionic operators above. However, in performing this expansion, we have expanded the dimension of the Hilbert space. The fermion operators act on a 2d so-called physical Hilbert space $\mathcal{H}$ (i.e. spin up and spin down), while the Majorana operators act on a 4d extended Hilbert space $\tilde{\mathcal{H}}$. Only the physical Hilbert space corresponds to observables, and the extended space is partially redundant, analogous to a gauge field. We restrict the extended space to the original space by imposing the physicality constraint that $|\psi\rangle \in \mathcal{H}$ if and only if $D|\psi\rangle = |\psi\rangle$ where $D = b^x b^y b^z c$ which we will not further discuss. There are many representations of the physical Pauli operators in terms of operators $\tilde{\sigma}^x, \tilde{\sigma}^x, \tilde{\sigma}^x$on the extended space, but they must satisfy a couple of conditions. First, they must preserve the physical space $\mathcal{H} \subset \tilde{\mathcal{H}}$ and must obey the same algebraic relations as the physical Pauli operators. We use the Majorana operators defined earlier to construct the representation

$$\tilde{\sigma}^x = ib^x c, \qquad \tilde{\sigma}^y = ib^y c, \qquad \tilde{\sigma}^z = ib^z c. \tag{12}$$

It is a simple exercise to show that these operators satisfy the necessary conditions. For multi-spin systems, we generalize the above construction to define the extended Pauli operators $\tilde{\sigma}^\alpha_j = ib^\alpha_j c_j$ and require that $|\psi\rangle \in \mathcal{H}$ if and only if $D_j|\psi\rangle = |\psi\rangle$ for all j where $D_j = b^x_j b^y_j b^z_j c_j$. This transformation from spin operators to (Majorana) fermion operators is contained in a more general class known as Jordan-Wigner transformations. We can now rewrite any multi-spin Hamiltonian in terms of Majorana fermion operators. We apply this result to the Kitaev Hamiltonian to obtain

$$\tilde{H} = \frac{i}{4}\sum_{j,k} \hat{A} c_j c_k, \qquad \hat{A}_{jk} = \begin{cases} 2J_{\alpha_{jk}}\hat{u}_{jk} & \text{if } j \text{ and } k \text{ are connected} \\ 0 & \text{else.} \end{cases} \tag{13}$$

where $\hat{u}_{jk} = ib^{\alpha_{jk}}_j b^{\alpha_{jk}}_k$. The problem is still not quite solved since this Hamiltonian does not appear much nicer than the one we started with. However, the crucial tool we now have at our disposal is that $[\hat{u}_{jk}, \hat{u}_{mn}] = 0$ and $[H, \hat{u}_{jk}] = 0$ for all j, k, m, n and so the extended space $\tilde{\mathcal{H}}$ can be decomposed into the eigenspaces of $\hat{u}_{jk}$, or $\tilde{\mathcal{H}} = \bigoplus_{[u]} \tilde{\mathcal{H}}_{[u]}$. If we then restrict the Hamiltonian to a particular sector (eigenspace), we obtain $\tilde{H}_u = \frac{i}{4}\sum_{j,k} A_{jk} c_j c_k$ where we have replaced the $\hat{A}$ operator with its evaluation A since u_{jk} is a scalar (the eigenvalue) when restricting to a sector. Hence we are left with a Hamiltonian which is quadratic in terms of Majorana fermion operators.

3.3 Energy spectrum

We now explore the ground state of this configuration. By construction, the ground state is contained (completely) in one of the u sectors, but it is not clear which one in particular. It turns out (non-trivial) that the ground state is located in the so-called vortex-free (vortex refers to a $w_= -1$ plaquette) sector where $w_p = 1$ for all plaquettes p as proved by Lieb. This sector has the property that $u_{jk} = 1$ for all links (j, k) so that j, k belongs to the A, B sublattice respectively. This realization is crucial. The sector containing the ground state is translationally invariant (or more precisely the set of bonds are invariant up to some discrete translations), and therefore we are invited to use the arsenal of Fourier analysis to tackle the problem of computing the energy spectrum. We change our notation and denote the site index j as (s, λ) where s denotes a unit cell and $\lambda = 0, 1$ to a (sub-)lattice site in the unit cell. As in the case of computing the energy spectrum of a tight-binding model, we define the Fourier transform of the creation and annihilation operators.

$$a_{\mathbf{k},\lambda} = \frac{1}{\sqrt{2N}}\sum_s e^{-i\mathbf{k}\cdot\mathbf{r}_s} c_{s\lambda} \tag{14}$$

where N is the total number of unit cells. We can use the inverse Fourier transform of the above to rewrite the Hamiltonian in momentum space as

$$H = \frac{1}{2} \sum_{\mathbf{k},\mu,\nu} iA_{\mu\nu}(\mathbf{k}) a_{-\mathbf{k},\mu} a_{\mathbf{k},\nu}, \qquad A_{\mu\nu}(\mathbf{k}) = \sum_t e^{i\mathbf{k}\cdot\mathbf{r}_t} A_{0\mu,t\nu}. \tag{15}$$

We can write A as a matrix in the basis $\{\mathbf{n}_1 = \frac{1}{2}(1, \sqrt{3}), \mathbf{n}_2 = \frac{1}{2}(-1, \sqrt{3})\}$ to obtain

$$iA(\mathbf{q}) = \begin{pmatrix} 0 & if(\mathbf{k}) \\ -if(\mathbf{k})^* & 0 \end{pmatrix}, \qquad f(\mathbf{k}) = 2(J_x e^{i\mathbf{k}\cdot\mathbf{n}_1} + J_y e^{i\mathbf{k}\cdot\mathbf{n}_2} + J_z) \tag{16}$$

with energy spectrum (eigenvalues) $\varepsilon(\mathbf{k}) = \pm|f(\mathbf{k})|$ for the conduction and valence bands respectively. This energy spectrum is very similar to that of a tight-binding model of graphene (with unequal bond tunnelling amplitudes), $\varepsilon(\mathbf{k}) = \pm|f(\mathbf{k})|$ where $f(\mathbf{k}) = \sum_{i=x,y,z} t_i e^{i\mathbf{k}\cdot\boldsymbol{\tau}_i}$ where $\boldsymbol{\tau}_i$ are the nearest-neighbor hopping vectors. However, unlike the spectrum of graphene which describes Dirac fermions (electrons), that of the Kitaev honeycomb model describes Majorana fermions. Remarkably, we have reduced the problem of interacting spins to that of non-interacting (a tight-binding-like model) Majorana fermions. We now study the dependence of the energy spectrum on the J parameters. More specifically, we are interested in when the spectrum is gapless (there exists a finite gap between the ground state and the first excited state) which in the present case corresponds to whether $\varepsilon(\mathbf{k}) = 0$ for some $\mathbf{k}$. It turns out that $\varepsilon(\mathbf{k})$ has solutions if and only if $|J_i| \leq |J_j| + |J_k|$ for all i, j, k not equal. If the inequality is saturated, then there are 2 solutions $\mathbf{k} = \pm\mathbf{k}^*$, and there is 1 solution otherwise.

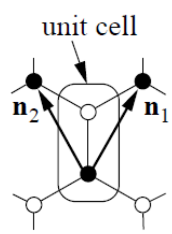

Figure 9: The unit cell in momentum space where $\mathbf{n}_1$ and $\mathbf{n}_2$ are identified [2].

There are 4 distinct phases, A_i for $i = x, y, z$ denoting to the 3 gapped phases, and B denoting the gapless phase. The gapped phases are algebraically distinct from one another. There are 8 versions of the gapless phases corresponding to the sign choices of the J parameters (e.g. $(J_x, J_y, J_z) = (\pm1, \pm1, \pm1)$) since these leave the inequality unchanged. In the gapless phase and with the strict inequality, the energy spectrum appears as a cone near the 2 $\varepsilon(\mathbf{k}) = 0$ solutions. Although there is not much information theory in the above discussion, it turns out that there are abelian and non-abelian anyons hiding in the phases which we will now explore.

3.4 Abelian anyons

We now discuss the A_z phase and derive that its excitations are abelian anyons. We could equivalently choose the other gapped phases A_x, A_y, but we focus on A_z for concreteness. Recall that the A_z phase is characterized by the condition that $|J_x| + |J_y| < |J_z|$. We restrict to the essential physics by taking the limit of small coupling $|J_x|, |J_y| \ll |J_z|$, without explicitly setting them to 0 since that would then correspond to the B phase. The Hamiltonian can now be decomposed as the

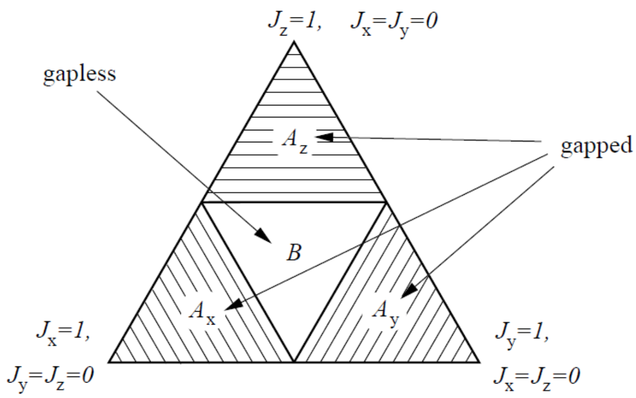

Figure 10: The phase diagram of the Kitaev honeycomb model showing the dependence on the J parameters. The A phases are gapped while the B phase is gapless [2].

J_z contribution H_0 and the perturbation V, or

$$H = H_0 + V, \qquad H_0 = -J_z \sum_{z \text{ links}} \sigma_j^z \sigma_k^z, \qquad V = -J_x \sum_{x \text{ links}} \sigma_j^x \sigma_k^x - J_y \sum_{y \text{ links}} \sigma_j^y \sigma_k^y. \tag{17}$$

Without loss of generality, we assume $J_z > 0$ and use perturbation theory to derive the effective Hamiltonian

$$H_{\text{eff}} = -J_{\text{eff}} \sum_p Q_p, \qquad J_{\text{eff}} = \frac{J_x^2 J_y^2}{16|J_z|^2}, \qquad Q_p = \sigma^y_{\text{left}(p)} \sigma^y_{\text{right}(p)} \sigma^z_{\text{up}(p)} \sigma^z_{\text{down}(p)}. \tag{18}$$

To recap, we started out with a hexagonal lattice and considered weak x, y links relative to z links. We then considered the essential physics of this system and used perturbation theory to find the effective Hamiltonian. The resulting effective lattice is a rhombus. We now map this rhombus to a square by rewriting the Hamiltonian in terms of the basis $\{\mathbf{m}_1 = \mathbf{n}_1 - \mathbf{n}_2, \mathbf{m}_2 = \mathbf{n}_1 + \mathbf{n}_2\}$ to obtain

$$H_{\text{eff}} = -J_{\text{eff}} \left(\sum_s Q_s + \sum_p Q_p \right) \tag{19}$$

where the first, second sum is carried out over vertices, plaquettes of the new lattice respectively. We can then apply a unitary transformation to obtain the final Hamiltonian

$$H'_{\text{eff}} = -J_{\text{eff}} \left(\sum_s A_s + \sum_p B_p \right). \tag{20}$$

where we omit the expressions for A_s and B_p for brevity although we note that $[A_s, B_p] = [A_i, A_j] = [B_i, B_j] = 0$ for all s, p, i, j. This immediately implies that the ground state $|\psi\rangle$ minimizes each term individually, or $A_s |\psi\rangle = +1 |\psi\rangle$ and $B_p |\psi\rangle = +1 |\psi\rangle$ for all vertices s and plaquettes p. Excited states correspond to flipping some of the plaquettes and/or vertices to -1. We refer to states which have a -1 eigenvalue of A_s for some vertex s as electric charges (e), and states which have a -1 eigenvalue of B_p for some plaquette p as magnetic vortex (m). We now study the fusion rules of these excitations. The model consists of 4 particles: the vacuum 1, electric charge e, magnetic vortex m, and fermion $\varepsilon = e \times m$. The fusion rules can be computed

$$e \times e = m \times m = \varepsilon \times \varepsilon = 1, \qquad e \times m = \varepsilon, e \times \varepsilon = m, \qquad m \times \varepsilon = e. \tag{21}$$

It turns out that e gain a trivial phase of 1 when braiding with itself (so it acts bosonic with respect to itself), but gains a phase of -1 when braiding with m. Similarly, m is also a boson. Also, m and e can fuse together to form a fermion ε. Braiding ε with e or m gains a phase of -1. These anyons are clearly abelian since each fusion channel has a single outcome. The ε fermions correspond to the fermions in the original model, though they are not the composite object of e and m. Also, e and m both correspond to vortices that reside on alternating rows of plaquettes in the original model.

3.5 Ising anyons

We now consider the gapless B phase and motivate that its excitations are non-abelian anyons. We first note that since the energy spectrum is gapless, vortices (excitations of the vortex-free sector) do not have well-defined braiding statistics. In other words, braiding 2 vortices depends on the particular path chosen and is not well-defined without also considering the length between the pair of vortices. In addition, the contribution from the particular process is significant since it is proportional to the amount of time required to complete the braid, but the adiabatic requirement also requires that the braiding is done slowly. This system is not ideal for topological quantum computing, and we must gap the energy spectrum to ensure well-defined braiding statistics. More specifically, we must gap the system by introducing a perturbation which does not obey time-reversal symmetry (to open a gap). We introduce a homogenous, constant magnetic field $\mathbf{h} = (h_x, h_y, h_z)$ which couples to all spins on the lattice. The perturbation can be written

$$V = -\sum_j (h_x \sigma_j^x + h_y \sigma_j^y + h_z \sigma_j^z) \tag{22}$$

where the sum is performed over all vertices. The magnetic field components only couple to the corresponding spin links. Without loss of generality, we assume $J_x = J_y = J_z = J$ to simply the computation. We compute the effective Hamiltonian acting on the vortex-free sector (containing the ground state) using perturbation theory to obtain the first non-trivial leading (3^{rd}) order contribution

$$H_{\text{eff}}^{(3)} \approx -\kappa \sum_{j,k,l} \sigma_j^x \sigma_k^y \sigma_l^z, \qquad \kappa = \frac{h_x h_y h_z}{J^2} \tag{23}$$

where the sum is performed over 2 particular arrangements of links. Rewriting the Hamiltonian by imposing this condition explicitly, we have

$$H_{\text{eff}} = \frac{i}{4} \sum_{j,k} A_{jk} c_j c_k \tag{24}$$

where we omit the expression of A for brevity, but its Fourier transform can be written as

$$iA(\mathbf{k}) = \begin{pmatrix} \Delta(\mathbf{k}) & if(\mathbf{k}) \\ -if(\mathbf{k}) & -\Delta(\mathbf{k}) \end{pmatrix}, \qquad \Delta(\mathbf{k}) \propto \kappa \tag{25}$$

from which we can compute the energy spectrum $\varepsilon(\mathbf{k}) = \sqrt{|f(\mathbf{k})|^2 + \Delta(\mathbf{k})^2}$. It is clear that $\Delta \propto \kappa$ determines the energy gap. Now that the energy spectrum is gapped for $\kappa \neq 0$, the braiding statistics of excitations (vortices) are well-defined assuming a few technical conditions. It turns out that the specific braiding rules of the vortices depend on a topological invariant known as the Chern number $\mathcal{C}$. We will not discuss the technicalities of the Chern number, but note that it captures the topological characteristic of eigenspaces and is an integer (similar to the genus of a 2-manifold). The Chern number cannot change due to continuous transformations of the parameter space that does not result in the closing or opening of a gap. For the gapped phases A_i, the Chern number is trivial, $\mathcal{C} = 0$. In the present case, if $\mathcal{C} = 1 \mod 2$ then vortices are non-abelian anyons. Physically, this phase corresponds to each vortex carrying an unpaired Majorana mode, but we will not discuss this notion further. The exact braiding statistics depends on $\mathcal{C} \mod 16$ and are derived using Conformal Field Theory (CFT) which is outside of the scope of this paper, although we refer the interested reader to [2]. Kitaev considers $\nu = 1$ and uses CFT to show that this simple example corresponds to the non-abelian Ising anyon model as we discussed earlier. Recall that the Ising anyon model consists of 3 particles $1, \sigma, \psi$ with the key non-abelian fusion channel $\sigma \times \sigma = 1 + \psi$ where in the present context σ is a vortex carrying an unpaired Majorana mode and ψ is a fermion.

4 Conclusion

We have discussed the Kitaev honeycomb model and its ability to host both abelian anyons and Ising non-abelian anyons, the latter of which can be used for universal topological quantum computation. The Hamiltonian was transformed from a system of interacting spins to that of non-interacting Majorana fermions through a Jordan-Wigner transformation. This model is interesting in its own right since the large number of conserved quantities (1 for each plaquette) allows us to reduce the problem size which is unlike other 2-dimensional spin-chains which are not exactly solvable by transformation to a fermion problem.

References

[1] Steven M. Girvin and Kun Yang. *Modern Condensed Matter Physics*. Cambridge University press, 2019.

[2] Alexei Kitaev. "Anyons in an exactly solved model and beyond". In: *Annals of Physics* 321.1 (2006), pp. 2–111. DOI: `10.1016/j.aop.2005.10.005`.

[3] Yingkai Liu. *Introduction to topological Quantum Computation: Ising anyons case study*. May 2019. URL: `https://yk-liu.github.io/2019/Introduction-to-QC-and-TQC-Ising-Anyons/`.

[4] Jiannis K Pachos. *Introduction to topological quantum computation*. Cambridge University Press, 2012.

This paper represents my own work in accordance with University regulations.
/s/ Amir Shapour Mohammadi